Quantum Spin Ice with Frustrated Transverse Exchange: From a π-Flux Phase to a Nematic Quantum Spin Liquid

Owen Benton,[1] L. D. C. Jaubert,[2] Rajiv R. P. Singh,[3] Jaan Oitmaa,[4] and Nic Shannon[5]
[1]*RIKEN Center for Emergent Matter Science (CEMS), Wako, Saitama 351-0198, Japan*
[2]*CNRS, Université de Bordeaux, LOMA, UMR 5798, 33400 Talence, France*
[3]*Department of Physics, University of California, Davis, California 95616, USA*
[4]*School of Physics, The University of New South Wales, Sydney 2052, Australia*
[5]*Okinawa Institute of Science and Technology Graduate University, Onna-son, Okinawa 904-0495, Japan*

(Received 26 February 2018; published 6 August 2018)

Quantum spin ice materials, pyrochlore magnets with competing Ising and transverse exchange interactions, have been widely discussed as candidates for a quantum spin-liquid ground state. Here, motivated by quantum chemical calculations for Pr pyrochlores, we present the results of a study for frustrated transverse exchange. Using a combination of variational calculations, exact diagonalization, numerical linked-cluster and series expansions, we find that the previously studied $U(1)$ quantum spin liquid, in its π-flux phase, transforms into a nematic quantum spin liquid at a high–symmetry, $SU(2)$ point.

DOI: 10.1103/PhysRevLett.121.067201

Pyrochlore magnets have proved to be a rich source of new phenomena [1,2], including the classical spin liquid "spin ice" [3,4], celebrated for its magnetic monopoles [5]. Pyrochlores are also central to the search for quantum spin liquids (QSL), massively entangled quantum phases of matter, which provide accessible examples of exotic, topological (quasi)particles previously studied in high-energy physics [6–9]. In particular, the quantum analogue of spin ice is known to support a three-dimensional QSL with fractional excitations, described by a $U(1)$ gauge theory [10–15], and has been vigorously pursued in experiment [16–21].

Exciting as these theoretical developments are, the range of experimental outcomes is far broader [1,2]. Encouragingly, studies of more general pyrochlore-lattice models, in their classical limit, reveal several new ordered and spin-liquid phases [18,22–25]. However, little is known about the ground state of even the simplest model of a quantum spin ice for frustrated transverse exchange, where quantum Monte Carlo (QMC) simulation fails [26,27]. Since microscopic estimates for Pr-based pyrochlores have predicted frustrated interactions [22], this is a question of fundamental and experimental interest.

In this Letter, we address the fate of the QSL in a quantum spin ice with frustrated transverse exchange. We find that the $U(1)$ QSL, in its π-flux phase [26], gives way to a new, nematic QSL, at an $SU(2)$-symmetry point in parameter space. The nematic QSL phase combines the symmetry fractionalization and emergent gauge degrees of freedom of spin liquids [7], with broken spin rotation symmetry, expressed through a bond-centered nematic order parameter [28]. The existence of the nematic QSL is supported by exact diagonalization (ED), cluster mean-field theory (CMFT), cluster-variational calculations (CVAR), and an exact, variational argument at the $SU(2)$ point. Evidence for the growth of nematic correlations, and an unusual scaling of the heat capacity at high temperature, is presented through numerical linked-cluster expansion (NLCE) and high-temperature expansion (HTE) calculations. These results provide an example of a nematic QSL [29] in three dimensions, confirming that pyrochlore

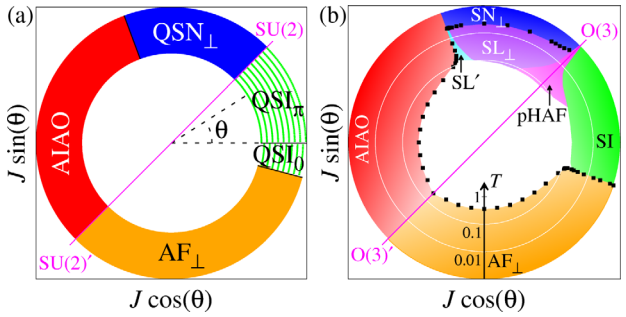

FIG. 1. Phase diagram of the quantum spin ice model $\mathcal{H}_{XXZ}$ [Eqs. (1) and (2)]: (a) Quantum phase diagram found in cluster-variational calculations for $T = 0$. Quantum spin liquids descended from spin ice, QSI_0 and QSI_π, compete with easy-plane antiferromagnetic order ($\mathrm{AF}_\perp$); all-in all-out order (AIAO); and a nematic QSL ($\mathrm{QSN}_\perp$). QSI_π and $\mathrm{QSN}_\perp$ are connected through an $SU(2)$-symmetric point. (b) Phase diagram found in classical Monte Carlo simulations for $T > 0$ (cf. Ref. [25]). Three spin liquids; spin ice (SI); the easy-plane spin liquid ($\mathrm{SL}_\perp$); and a pseudo-Heisenberg antiferromagnet (PHAF), compete with a nematic spin liquid ($\mathrm{SN}_\perp$), and $\mathrm{AF}_\perp$ and AIAO order. An additional disordered regime (SL′) shares the correlations of $\mathrm{SL}_\perp$ and AIAO. The white circles indicate the radial, logarithmic, temperature scale. Simulation details are given in the Supplemental Materials [30].

magnets can support a range of different QSL ground states and are summarized in Fig. 1.

We consider the spin-1/2 XXZ Hamiltonian on the pyrochlore lattice

$$\mathcal{H}_{XXZ} = \sum_{\langle ij \rangle} [J_{zz} \mathsf{S}_i^z \mathsf{S}_j^z - J_{\pm}(\mathsf{S}_i^+ \mathsf{S}_j^- + \mathsf{S}_j^+ \mathsf{S}_i^-)], \quad (1)$$

where spin coordinates are defined locally such that the z axis of spin space is aligned with a local C_3 axis [16,24]. Equation (1) can be derived from atomic models of pyrochlore oxides [22,37,38] and, for $J_{zz} \gg J_{\pm} > 0$, has been studied as a minimal model of a quantum spin ice [10–15,26,27,39–46]. We set

$$J_{zz} = J\cos\theta, \qquad J_{\pm} = -\frac{J}{2}\sin\theta. \quad (2)$$

At $\theta = \pi/4$, and $\theta = -3\pi/4$, $\mathcal{H}_{XXZ}$ is equivalent to a Heisenberg model, with $SU(2)$ symmetry.

For unfrustrated interactions, $-\pi < \theta < 0$, $\mathcal{H}_{XXZ}$ [Eq. (1)] is accessible to QMC calculations. For $\theta \lesssim 0$, the ground state is a $U(1)$ QSL (QSI_0), giving way to easy-plane antiferromagnetism ($\mathrm{AF}_\perp$) for $\theta < -0.033\pi$ [11,12,14]. Perturbative arguments imply that the $U(1)$ QSL survives for frustrated interactions, $\theta \gtrsim 0$ [10]. In this case, the $U(1)$ QSL enters a "π-flux phase" (QSI_π), with fractionalized translational symmetry [26,27]. Classical Monte Carlo simulations suggest that $\mathcal{H}_{XXZ}$ remains in a spin liquid state for $0 < \theta < 0.602\pi$, but that this spin liquid changes character traversing the high-symmetry point $\theta = \pi/4$ [25]—cf. Fig. 1(b). The fate of the quantum, π-flux ground state, however, remains unknown.

Cluster mean-field theory.—To illuminate this question, first, we explore the ground state of $\mathcal{H}_{XXZ}$ [Eq. (1)] within CMFT. CMFT consists in breaking the lattice up into finite clusters, treating interactions within each cluster exactly, and those between clusters at a mean-field level [47–51]. The geometry of the pyrochlore lattice permits degenerate CMFT solutions, with translational symmetry restored, in contrast to some previous approaches (see, e.g., [52]), allowing treatment of spin liquids.

We start by dividing the pyrochlore lattice into two sublattices of tetrahedra, "A" and "B", and writing the wave function as a product over A tetrahedra

$$|\psi^{\mathrm{CMFT}}(\{\mathbf{h}\})\rangle = \Pi_{t\in A}|\phi_t(\{\mathbf{h}\})\rangle, \quad (3)$$

where $|\phi_t(\{\mathbf{h}\})\rangle$ is defined as the ground state of an auxiliary Hamiltonian on tetrahedron t

$$\mathcal{H}'(t) = \mathcal{H}_{XXZ}(t) - \sum_{i\in t} \mathbf{h}_i \cdot \mathsf{S}_i. \quad (4)$$

The fields $\{\mathbf{h}\}$ are variational parameters, chosen to minimize

$$E_{\mathrm{CMFT}} = \langle \psi^{\mathrm{CMFT}}(\{\mathbf{h}\})|\mathcal{H}_{XXZ}|\psi^{\mathrm{CMFT}}(\{\mathbf{h}\})\rangle. \quad (5)$$

The corner-sharing geometry of the lattice permits single tetrahedron solutions to be connected in many different ways (cf. "lego-brick rules" in [24]). For this reason, the solutions for $\{\mathbf{h}\}$, and the corresponding wave functions $|\psi^{\mathrm{CMFT}}(\{\mathbf{h}\})\rangle$, encompass both disordered and ordered states.

We find four kinds of optimal solutions for $\mathbf{h}_i$, each corresponding to a different region of the phase diagram Fig. 1(a). For $0.613\pi \lesssim \theta < 5\pi/4$, the optimal solution has $\mathbf{h}_i = h\hat{\mathbf{z}}$ everywhere, corresponding to all-in, all-out (AIAO) order. For $-(3\pi/4) < \theta \lesssim -0.081\pi$, fields $\mathbf{h_i}$ are ordered in the local xy plane, with (e.g.,) $\mathbf{h}_i = h\hat{\mathbf{x}}$. This is the easy-plane antiferromagnet, $\mathrm{AF}_\perp$.

For $-0.081\pi \lesssim \theta < (\pi/4)$, the solutions are spin-ice-like. The fields $\mathbf{h}_i$ have the form $\mathbf{h}_i = \sigma_i h\hat{\mathbf{z}}$, where $\sigma_i = \pm 1$. The minimum value of E_{CMFT} is attained by any configuration of σ_i with two plus signs and two minus signs on every tetrahedron. It is known that quantum tunneling between spin-ice configurations results in two distinct $U(1)$ QSLs, depending on the sign of $J_\pm$ [26,27]. These two phases, QSI_0 and QSI_π, cannot be distinguished within CMFT but are distinguishable using the variational approach discussed below.

For $(\pi/4) \lesssim \theta < 0.613\pi$, the solutions are similar to the spin-ice case but now have the fields $\mathbf{h}_i$ lying collinearly in the xy plane, e.g., $\mathbf{h}_i = \sigma_i h\hat{\mathbf{x}}$. Once again, E_{CMFT} is minimized by any configuration of σ_i with two plus signs and two minus signs on every tetrahedron. Since these σ_i are disordered, the resulting state does not possess conventional magnetic order. Nevertheless, the selection of a global axis in the xy plane implies breaking of the $U(1)$ spin-rotation symmetry of Eq. (1). This results in a finite value of the spin-nematic order parameter

$$\mathcal{Q}_\perp = \left\langle \frac{1}{3N} \sum_{\langle ij \rangle} \begin{pmatrix} \mathsf{S}_i^x \mathsf{S}_j^x - \mathsf{S}_i^y \mathsf{S}_j^y \\ \mathsf{S}_i^x \mathsf{S}_j^y + \mathsf{S}_i^y \mathsf{S}_j^x \end{pmatrix} \right\rangle, \quad (6)$$

defined on the bonds $\langle ij \rangle$ of the lattice [25].

Cluster-variational calculations.—The CMFT wave function, Eq. (3), is entangled at the level of a single tetrahedron, and can describe disordered and ordered states. But it cannot capture the long-range entanglement of a QSL. Thus, distinguishing the quantum ground states of Eq. (1) requires going beyond CMFT. For this, we introduce the CVAR approach, based on a coherent superposition of the degenerate wave functions found in CMFT. We apply it to the case where CMFT predicts spin-nematic order, finding that fluctuations beyond CMFT lead to a nematic $U(1)$ QSL (see Supplemental Material [30]).

We begin with the CMFT result for a spin-nematic state with collinearity axis $\mathbf{h} \| \hat{\mathbf{x}}$. We consider a superposition of CMFT solutions

$$|\varphi\rangle = \sum_{\{\sigma\}} a_{\{\sigma\}} |\psi^{\mathrm{CMFT}}(h\sigma_i \hat{\mathbf{x}})\rangle, \tag{7}$$

where the sum runs over all Ising configurations $\{\sigma\}$ with two plus and two minus signs on every tetrahedron. The coefficients $a_{\{\sigma\}}$ are variational parameters to optimize the energy

$$E_{\mathrm{CVAR}} = \frac{\langle\varphi|\mathcal{H}_{XXZ}|\varphi\rangle}{\langle\varphi|\varphi\rangle}. \tag{8}$$

The wave functions $|\psi^{\mathrm{CMFT}}(h\sigma_i\hat{\mathbf{x}})\rangle$ labeled by different configurations $\{\sigma\}$ are not generally orthogonal. Their overlap can be parametrized by the overlaps between different CMFT wave functions $|\phi_t(\mathbf{h})\rangle$ on a single tetrahedron. The overlap between two optimized CMFT wave functions scales as $\sim o_2^{n_2} o_4^{n_4}$ where n_m is the number of A tetrahedra on which the arrangement of σ_i differs by m sites, and $o_m(\theta)$ is the corresponding overlap of wave functions within a single tetrahedron. By expanding Eq. (8) in powers of o_2 and o_4, we can derive an effective Hamiltonian $\mathbf{H}_{\mathrm{eff}}$ acting amongst CMFT states. The leading term in $\mathbf{H}_{\mathrm{eff}}$ is a ring exchange term $g_6 \sim o_2^2$, which reverses the signs of σ_i around six-bond loops in the lattice. Higher order corrections to $\mathbf{H}_{\mathrm{eff}}$ are also ring exchanges with size decreasing exponentially with the length of the ring. The next-to-leading terms involving eight-bond ring exchange are substantially smaller than g_6 throughout the region $(\pi/4) < \theta < 0.613\pi$. The ratio of eight-bond to six-bond ring exchanges is smallest ($\sim$0.18) bordering the AIAO phase.

The ground state favored by the six-bond ring exchange has been studied using QMC calculations in [12], finding a $U(1)$ QSL. Therefore, we expect that, near to the AIAO phase, where g_6 is more than 5 times larger than higher order terms, the optimal superposition of CMFT states [Eq. (7)], is also a $U(1)$ QSL. Since each CMFT state has the same value of $\mathcal{Q}_\perp$ [Eq. (6)], this QSL retains spin-nematic order. Following [29], we dub this phase a "nematic quantum spin liquid," denoting it $\mathrm{QSN}_\perp$ in Fig. 1(a). Below, we present independent arguments which establish the relevance of $\mathrm{QSN}_\perp$ near the Heisenberg point and provide further support for nematicity bordering the AIAO phase.

While the breaking of $U(1)$ spin rotation symmetry in the phase $\mathrm{QSN}_\perp$ is the most obvious difference between $\mathrm{QSN}_\perp$ and QSI_π, the two phases can be distinguished in the absence of this symmetry if certain other symmetries are present. If $U(1)$ symmetry is broken down to C_3 by anisotropic exchange (as in Pr pyrochlores), then $\mathrm{QSN}_\perp$ still breaks the C_3 symmetry, and is a distinct phase. If there is only π rotation symmetry around the z axis of spin space, then $\mathrm{QSN}_\perp$ loses its symmetry breaking character and ceases to be a true nematic phase. However, it remains distinguishable from QSI_π by the quantum numbers of its photon excitations. In QSI_π the emergent electric field associated with the photons is invariant under π rotations around the z axis of spin space ($E \to E$), whereas in $\mathrm{QSN}_\perp$, it reverses its sign ($E \to -E$). Therefore, in this case, $\mathrm{QSN}_\perp$ remains distinct from QSI_π, despite no longer breaking a symmetry of the Hamiltonian.

Further support for nematic order.—Now, we provide two further arguments supporting spin-nematic order.

The first argument is based on approaching the $SU(2)$ point $\theta = (\pi/4)$ from the small θ side. For small $\theta > 0$, the ground state is the π-flux $U(1)$ QSL [10,26,27] [QSI_π in Fig. 1(a)]. Gauge mean field theory predicts this state to be stable up to $\theta \approx 0.46\pi$ [26], well beyond the $SU(2)$ point. However, we show that, at the $SU(2)$ point, it must become unstable to nematicity.

To see this, observe that a wave function for the spin-nematic phase can be generated by taking a ground state wave function from within the QSI_π phase and acting on it with global spin rotations

$$|\mathrm{nem}(\psi)\rangle = \mathcal{R}_z(\psi)\mathcal{R}_y\left(\frac{\pi}{2}\right)|\mathrm{QSI}_\pi\rangle, \tag{9}$$

where $\mathcal{R}_\alpha(\phi)$ denotes a global rotation by an angle ϕ, around the α axis of spin space. $|\mathrm{nem}(\psi)\rangle$ generically supports a finite value of the nematic bond order parameter $\mathcal{Q}_\perp$ [Eq. (6)], with all dipolar expectation values vanishing. ψ parametrizes the direction of $\mathcal{Q}_\perp$ in the nematic state.

Global $SU(2)$ rotations become symmetries of the model at $\theta = (\pi/4)$. Thus, if QSI_π is stable up to the $SU(2)$ point, the energy gap to the nematic state must vanish, indicating a nematic instability. It follows that the resulting spin-nematic state inherits the gauge structure and symmetry fractionalization of QSI_π.

The above argument cannot rule out some other ground state taking over from QSI_π before $\theta = (\pi/4)$. Such alternative states around $\theta = (\pi/4)$ could include various dimer-ordered [53–57] and spin-liquid [58–61] states, although the mean field energy of a valence bond covering of the lattice is higher than the mean field energy of $\mathrm{QSN}_\perp$ and QSI_π at $\theta = (\pi/4)$. It is useful, therefore, to have an alternative way to establish nematic order. This is provided by considering the excitations of the AIAO phase found for $J_{zz} < 0$ [cf. Fig. 1(a)].

The AIAO state is the polarized state with maximum total S^z. Since S^z is conserved, excitations can be labeled by the number of spin flips, δS^z relative to this state.

An instability to conventional XY ordering would be indicated by the softening of a $\delta S^z = 1$ excitation (magnon). An instability to nematic order, by contrast, is indicated by the softening of a $\delta S^z = 2$ excitation: a two-magnon bound state [28].

For $\sin(\theta) > 0$, the lowest energy state with $\delta S^z = 1$ has a gap $\Delta(\delta S^z = 1) = J[-3\cos(\theta) - \sin(\theta)]$.

In Fig. 2, this is compared with the lowest energy state of the $\delta S^z = 2$ sector, calculated using ED on a 128-site cubic

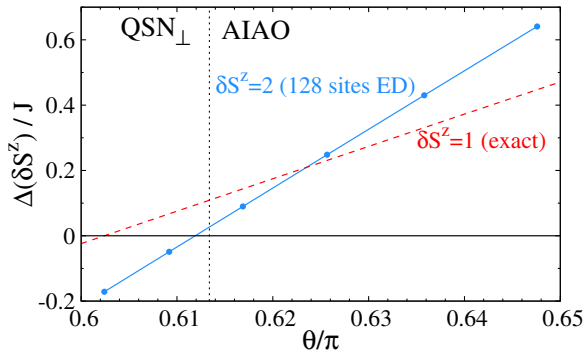

FIG. 2. Condensation of two-magnon bound states within the AIAO phase, indicating the onset of spin-nematic order. Gaps to the lowest one-magnon and two-magnon excitations of the AIAO phase, $\Delta(\delta S^z = 1)$ and $\Delta(\delta S^z = 2)$, are shown as a function of the Hamiltonian parameter θ [Eq. (2)]. For $\delta S^z = 1$, the gap is exact, while for $\delta S^z = 2$, it is estimated numerically for a 128 site cluster. As θ decreases towards $\theta = 0.612\pi$ the two-magnon state comes below the one magnon state and then condenses. The condensation of two-magnon bound states indicates incipient nematicity [28]. The resultant phase boundary between $\mathrm{QSN}_\perp$ and AIAO, $\theta \approx 0.612\pi$, is close to that found in CVAR $\theta \approx 0.613\pi$ [cf. Fig. 1(a)], shown as a dashed line.

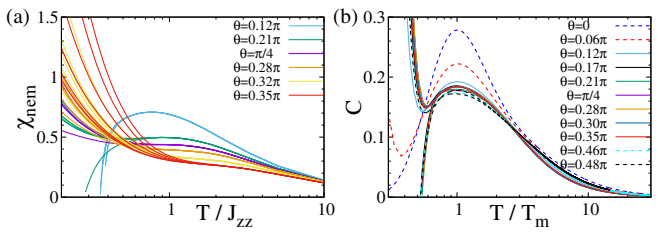

FIG. 3. Finite-temperature properties of frustrated quantum spin ice [Eq. (1)]. (a) Susceptibility $\chi_{\mathrm{nem}}(T)$ associated with spin-nematic order [Eq. (6)], from HTE. Temperature in (a) is shown in units of the Ising exchange $J_{zz} = J\cos(\theta)$. Different curves for a given value of θ correspond to different Padé approximants. For $\theta > (\pi/4)$, $\chi_{\mathrm{nem}}(T)$ shows an upturn at low temperatures, consistent with an approach to spin-nematic order. (b) Heat capacity C, as a function of reduced temperature T/T_m, calculated within NLCE. Here, T_m is the temperature of the heat capacity maximum; different curves for the same θ represent different orders of NLCE; agreement between these indicates convergence. Plots of $C(T/T_m)$ collapse onto one another for $\theta \gtrsim 0.17\pi$, consistent with an extended regime where finite-temperature properties are controlled by the zero-temperature $SU(2)$ point $\theta = (\pi/4)$, reminiscent of quantum criticality.

cluster with periodic boundary conditions. Approaching the boundary of the AIAO phase, the $\delta S^z = 2$ gap comes below that for $\delta S^z = 1$, indicating formation of a two-magnon bound state with lower energy than the lowest single-magnon state. The two-magnon gap closes at $\theta \approx 0.612\pi$, indicating an instability to nematic order, in good agreement with $\theta \approx 0.613\pi$ found using CVAR [Fig. 1(a)].

Finite temperature.—Thus far, we have presented evidence for a nematic $U(1)$ QSL phase at $T = 0$. In simulations of the corresponding classical model, nematic order arises at temperatures $T \sim 10^{-2}J$ [Fig. 1(b)]. This is similar to the energy scale of collinear ground state selection in CMFT, suggesting a comparable transition temperature in the quantum model. This raises the question of what would be observed in a spin ice with frustrated transverse exchange at intermediate temperatures $T \sim J$.

To address this, we turn to series expansion methods. Specifically, we use HTE [62–64] and NLCE [64–66] to calculate the nematic susceptibility $\chi_{\mathrm{nem}}(T)$ and heat capacity $C(T)$ (see Supplemental Material [30]). We focus on parameters near the $SU(2)$ point $\theta = (\pi/4)$, where our theory predicts a zero-temperature phase transition between QSI_π and $\mathrm{QSN}_\perp$. This point was recently studied using diagrammatic Monte Carlo calculations [67], finding spin-ice-like correlations down to $T = J/6$, consistent with our CVAR results.

HTE of the nematic susceptibility $\chi_{\mathrm{nem}}(T)$ is plotted in Fig. 3(a), for various exchange parameters. HTE converges down to $T \sim J$, which is not low enough to see any definitive signature of nematic order. However, there is a hint of a low-temperature transition at $\theta = (\pi/4)$ in the behavior of Padé approximants of $\chi_{\mathrm{nem}}(T)$. For $\theta \lesssim (\pi/4)$, the Padé approximants indicate a suppression of the nematic susceptibility below $T \sim J$, whereas for $\theta > (\pi/4)$, they show an upturn at low temperatures. Future diagrammatic QMC studies may be able to track the growth of the nematic susceptibility down to lower temperatures than accessible in our series expansion results.

A further hint of interesting physics at the $SU(2)$ point is revealed in NLCE calculations of the heat capacity [Fig. 3(b)]. The calculations show a broad maximum at temperatures $T_m(\theta)$ just above the temperature where NLCE fails to converge. For a wide range of parameters around the $SU(2)$ point, the heat capacity curves for different values of θ can be collapsed onto one another by rescaling the temperature axis by $T_m(\theta)$.

This suggests a region of parameter space where the finite-temperature physics is controlled by a single point on the zero-temperature phase diagram. This is reminiscent of quantum criticality, consistent with the scenario of a zero-temperature transition between nematic and QSI_π phases at $\theta = (\pi/4)$.

Conclusions.—We have explored the properties of a minimal model of a quantum spin ice, the spin-1/2 XXZ model on the pyrochlore lattice $\mathcal{H}_{XXZ}$ [Eq. (1)], focusing on frustrated transverse exchange $J_\pm < 0$. We have determined the ground states of this model within a variational approach, CVAR, which builds upon the degenerate wave functions found in cluster mean field theory [Fig. 1(a)]. We find that a $U(1)$ QSL derived from spin ice, QSI_π, transforms into another $U(1)$ QSL with easy-plane character and spin-nematic order, $\mathrm{QSN}_\perp$, at the high-symmetry point, $J_\pm = -J_{zz}/2$. Further evidence for this phase transition

comes from an exact, variational argument, analysis of the two-magnon instability of the neighboring all-in, all-out phase [Fig. 2], and finite temperature thermodynamics [Fig. 3]. The variational approach introduced, CVAR, could be applied to other frustrated quantum models, where QMC calculations are unfeasible.

The nematic QSL, $QSN_{\perp}$, owns both the gauge degrees of freedom and topological excitations of a $U(1)$ QSL [10,13,15,26,43], and the Goldstone modes associated with broken spin-rotation symmetry (cf. [25,68]). Exactly how these excitations combine is a challenging open problem.

Our results offer new perspectives for experiment. Among the most promising candidates for realizing a quantum spin ice are Pr-based pyrochlores [17,19,21,69]. Our work is particularly relevant to this case, based on microscopic calculations of the sign of transverse exchange [22]. In light of this, Pr pyrochlores may be proximate to a nematic QSL, although the experimental situation is complicated by structural disorder, which opens up new routes to both QSL and non-QSL ground states [18,20,45,70–73].

We anticipate that $QSN_{\perp}$ can be identified through its gapped and gapless excitations, through the fractionalization of translation symmetry [26,43], and through pinch points in quasielastic neutron scattering [25], which would "wash out" at low temperatures [13]. It could be distinguished from QSI_{π} by the presence of a Goldstone mode, which would become gapped, but remain present in the spectrum, in the presence of exchange anisotropy. The $\mathbf{q}$ dependence of the intensity for photon excitations should also differ between $QSN_{\perp}$ and QSI_{π} because the emergent electromagnetic fields are associated with different spin components.

Given the developing experimental situation, with new pyrochlores continuing to be synthesized [74,75], a realization of a nematic QSL may not be too distant.

The authors are grateful to Judit Romhányi for a careful reading of the manuscript. This work was supported by the Theory of Quantum Matter Unit of the Okinawa Institute of Science and Technology Graduate University (OIST), and by the IdEx Bordeaux BIS–Helpdesk (L. J.). The work of R. R. P. S. is supported in part by the US National Science Foundation Grant No. DMR–1306048. O. B. and L. J. acknowledge the hospitality of OIST, where part of this work was completed.

[1] J. S. Gardner, M. J. P. Gingras, and J. E. Greedan, Magnetic pyrochlore oxides, Rev. Mod. Phys. **82**, 53 (2010).
[2] A. M. Hallas, J. Gaudet, and B. D. Gaulin, Experimental insights into ground state selection of quantum XY pyrochlores, Annu. Rev. Condens. Matter Phys. **9**, 105 (2018).
[3] S. T. Bramwell and M. J. P. Gingras, Spin ice state in frustrated magnetic pyrochlore materials, Science **294**, 1495 (2001).
[4] C. Castelnovo, R. Moessner, and S. L. Sondhi, Spin ice, fractionalization, and topological order, Annu. Rev. Condens. Matter Phys. **3**, 35 (2012).
[5] C. Castelnovo, R. Moessner, and S. L. Sondhi, Magnetic monopoles in spin ice, Nature (London) **451**, 42 (2008).
[6] L. Balents, Spin liquids in frustrated magnets, Nature (London) **464**, 199 (2010).
[7] L. Savary and L. Balents, Quantum spin liquids: a review, Rep. Prog. Phys. **80**, 016502 (2017).
[8] Y. Zhou, K. Kanoda, and T. K. Ng, Quantum spin liquid states, Rev. Mod. Phys. **89**, 025003 (2017).
[9] M. R. Norman, Colloquium: Herbertsmithite and the search for the quantum spin liquid, Rev. Mod. Phys. **88**, 041002 (2016).
[10] M. Hermele, M. P. A. Fisher, and L. Balents, Pyrochlore photons: The U(1) spin liquid in a $S = \frac{1}{2}$ three-dimensional frustrated magnet, Phys. Rev. B **69**, 064404 (2004).
[11] A. Banerjee, S. V. Isakov, K. Damle, and Y. B. Kim, Unusual Liquid State of Hard-Core Bosons on the Pyrochlore Lattice, Phys. Rev. Lett. **100**, 047208 (2008).
[12] N. Shannon, O. Sikora, F. Pollmann, K. Penc, and P. Fulde, Quantum Ice: A Quantum Monte Carlo Study, Phys. Rev. Lett. **108**, 067204 (2012).
[13] O. Benton, O. Sikora, and N. Shannon, Seeing the light: Experimental signatures of emergent electromagnetism in a quantum spin ice, Phys. Rev. B **86**, 075154 (2012).
[14] Y. Kato and S. Onoda, Numerical Evidence of Quantum Melting of Spin Ice: Quantum-to-Classical Crossover, Phys. Rev. Lett. **115**, 077202 (2015).
[15] C.-J. Huang, Y. Deng, Y. Wan, and Z. Y. Meng, Dynamics of Topological Excitations in a Model Quantum Spin Ice, Phys. Rev. Lett. **120**, 167202 (2018).
[16] K. A. Ross, L. Savary, B. D. Gaulin, and L. Balents, Quantum Excitations in Quantum Spin Ice, Phys. Rev. X **1**, 021002 (2011).
[17] K. Kimura, S. Nakatsuji, J-J. Wen, C. Broholm, M. B. Stone, E. Nishibori, and H. Sawa, Quantum fluctuations in spin-ice-like $Pr_2Zr_2O_7$, Nat. Commun. **4**, 1934 (2013).
[18] S. Petit, E. Lhotel, S. Guitteny, O. Florea, J. Robert, P. Bonville, I. Mirebeau, J. Ollivier, H. Mutka, E. Ressouche, C. Decorse, M. Ciomaga Hatnean, and G. Balakrishnan, Antiferroquadrupolar correlations in the quantum spin ice candidate $Pr_2Zr_2O_7$, Phys. Rev. B **94**, 165153 (2016).
[19] J.-J. Wen, S. M. Koohpayeh, K. A. Ross, B. A. Trump, T. M. McQueen, K. Kimura, S. Nakatsuji, Y. Qiu, D. M. Pajerowski, J. R. D. Copley, and C. L. Broholm, Disordered Route to the Coulomb Quantum Spin Liquid: Random Transverse Fields on Spin Ice in $Pr_2Zr_2O_7$, Phys. Rev. Lett. **118**, 107206 (2017).
[20] N. Martin, P. Bonville, E. Lhotel, S. Guitteny, A. Wildes, C. Decorse, M. Ciomaga Hatnean, G. Balakrishnan, I. Mirebeau, and S. Petit, Disorder and Quantum Spin Ice, Phys. Rev. X **7**, 041028 (2017).
[21] R. Sibille, N. Gauthier, H. Yan, M. Ciomaga Hatnean, J. Ollivier, B. Winn, U. Filges, G. Balakrishnan, M. Kenzelmann, N. Shannon, and T. Fennell, Experimental signatures of emergent quantum electrodynamics in $Pr_2Hf_2O_7$, Nat. Phys. **14**, 711(2018).
[22] S. Onoda and Y. Tanaka, Quantum fluctuations in the effective pseudospin-$\frac{1}{2}$ model for magnetic pyrochlore oxides, Phys. Rev. B **83**, 094411 (2011).

[23] O. Benton, L. D. C. Jaubert, H. Yan, and N. Shannon, A spin-liquid with pinch-line singularities on the pyrochlore lattice, Nat. Commun. **7**, 11572 (2016).

[24] H. Yan, O. Benton, L. Jaubert, and N. Shannon, Theory of multiple-phase competition in pyrochlore magnets with anisotropic exchange with application to $Yb_2Ti_2O_7$, $Er_2Ti_2O_7$, and $Er_2Sn_2O_7$, Phys. Rev. B **95**, 094422 (2017).

[25] M. Taillefumier, O. Benton, H Yan, L. D. C. Jaubert, and N. Shannon, Competing Spin Liquids and Hidden Spin-Nematic Order in Spin Ice with Frustrated Transverse Exchange, Phys. Rev. X **7**, 041057 (2017).

[26] S. B. Lee, S. Onoda, and L. Balents, Generic quantum spin ice, Phys. Rev. B **86**, 104412 (2012).

[27] G. Chen, Spectral periodicity of the spinon continuum in quantum spin ice, Phys. Rev. B **96**, 085136 (2017).

[28] N. Shannon, T. Momoi, and P. Sindzingre, Nematic Order in Square Lattice Frustrated Ferromagnets, Phys. Rev. Lett. **96**, 027213 (2006).

[29] T. Grover, N. Trivedi, T. Senthil, and P. A. Lee, Weak Mott insulators on the triangular lattice: Possibility of a gapless nematic quantum spin liquid, Phys. Rev. B **81**, 245121 (2010).

[30] See Supplemental Material at http://link.aps.org/supplemental/10.1103/PhysRevLett.121.067201 for details of Monte Carlo, CMFT, CVAR, NLCE, and HTE calculations, which includes Refs. [31–36].

[31] D. S. Rokhsar and S. A. Kivelson, Superconductivity and the Quantum Hard-Core Dimer Gas, Phys. Rev. Lett. **61**, 2376 (1988).

[32] A. Ralko, M. Mambrini, and D. Poilblanc, Generalized quantum dimer model applied to the frustrated Heisenberg model on the square lattice: Emergence of a mixed columnar-plaquette phase, Phys. Rev. B **80**, 184427 (2009).

[33] G. A. Baker, Jr. and P. Graves-Morris, *Padé Approximants* (Cambridge University Press, Cambridge, England, 1996).

[34] M. Rigol, T. Bryant, and R. R. P. Singh, Numerical Linked-Cluster Approach to Quantum Lattice Models, Phys. Rev. Lett. **97**, 187202 (2006).

[35] N. R. Hayre, K. A. Ross, R. Applegate, T. Lin, R. R. P. Singh, B. D. Gaulin, and M. J. P. Gingras, Thermodynamic properties of $Yb_2Ti_2O_7$ pyrochlore as a function of temperature and magnetic field: Validation of a quantum spin ice exchange Hamiltonian, Phys. Rev. B **87**, 184423 (2013).

[36] R. R. P. Singh and J. Oitmaa, Corrections to Pauling residual entropy and single tetrahedron based approximations for the pyrochlore lattice Ising antiferromagnet, Phys. Rev. B **85**, 144414 (2012).

[37] H. R. Molavian, M. J. P. Gingras, and B. Canals, Dynamically Induced Frustration as a Route to a Quantum Spin Ice State in $Tb_2Ti_2O_7$ via Virtual Crystal Field Excitations and Quantum Many-Body Effects, Phys. Rev. Lett. **98**, 157204 (2007).

[38] S. Onoda and Y. Tanaka, Quantum Melting of Spin Ice: Emergent Cooperative Quadrupole and Chirality, Phys. Rev. Lett. **105**, 047201 (2010).

[39] L. Savary and L. Balents, Coulombic Quantum Liquids in Spin-1/2 Pyrochlores, Phys. Rev. Lett. **108**, 037202 (2012).

[40] Z. Hao, A. G. R. Day, and M. J. P. Gingras, Bosonic many-body theory of quantum spin ice, Phys. Rev. B **90**, 214430 (2014).

[41] P. A. McClarty, O. Sikora, R. Moessner, K. Penc, F. Pollmann, and N. Shannon, Chain-based order and quantum spin liquids in dipolar spin ice, Phys. Rev. B **92**, 094418 (2015).

[42] M. J. P. Gingras and P. A. McClarty, Quantum spin ice: A search for gapless quantum spin liquids in pyrochlore magnets, Rep. Prog. Phys. **77**, 056501 (2014).

[43] G. Chen, Magnetic monopole, condensation of the pyrochlore ice U(1) quantum spin liquid: Application to $Pr_2Ir_2O_7$ and $Yb_2Ti_2O_7$, Phys. Rev. B **94**, 205107 (2016).

[44] N. Shannon, in *Spin Ice*, edited by M. Udagawa and L. D. C. Jaubert (Springer, New York, to be published).

[45] L. Savary and L. Balents, Disorder-Induced Quantum Spin Liquid in Spin Ice Pyrochlores, Phys. Rev. Lett. **118**, 087203 (2017).

[46] G. Chen, Dirac's "magnetic monopoles", in pyrochlore ice $U(1)$ spin liquids: Spectrum and classification, Phys. Rev. B **96**, 195127 (2017).

[47] A. J. García-Adeva and D. L. Huber, Quantum Tetrahedral Mean Field Theory of the Magnetic Susceptibility for the Pyrochlore Lattice, Phys. Rev. Lett. **85**, 4598 (2000).

[48] A. J. García-Adeva and D. L. Huber, Quantum tetrahedral mean-field theory of the pyrochlore lattice, Can. J. Phys. **79**, 1359 (2001).

[49] N. Shannon, Mixed valence on a pyrochlore lattice—LiV_2O_4 as a geometrically frustrated magnet, Eur. Phys. J. B **27**, 527 (2002).

[50] D. Yamamoto, G. Marmorini, and I. Danshita, Quantum Phase Diagram of the Triangular-Lattice *XXZ* Model in a Magnetic Field, Phys. Rev. Lett. **112**, 127203 (2014).

[51] B. Javanparast, A. G. R. Day, Z. Hao, and M. J. P. Gingras, Order-by-disorder near criticality in *XY* pyrochlore magnets, Phys. Rev. B **91**, 174424 (2015).

[52] D. Yamamoto, G. Marmorini, and I. Danshita, Microscopic Model Calculations for the Magnetization Pocess of Layered Triangular-Lattice Quantum Antiferromagnets, Phys. Rev. Lett. **114**, 027201 (2015).

[53] A. B. Harris, A. J. Berlinsky, and C. Bruder, Ordering by quantum fluctuations in a strongly frustrated Heisenberg antiferromagnet, J. Appl. Phys. **69**, 5200 (1991).

[54] E. Berg, E. Altman, and A. Auerbach, Singlet Excitations in Pyrochlore: A Study of Quantum Frustration, Phys. Rev. Lett. **90**, 147204 (2003).

[55] H. Tsunetsugu, Antiferromagnetic quantum spins on the pyrochlore lattice, J. Phys. Soc. Jpn. **70**, 640 (2001).

[56] H. Tsunetsugu, Spin-singlet order in a pyrochlore antiferromagnet, Phys. Rev. B **65**, 024415 (2001).

[57] R. Moessner, S. L. Sondhi, and M. O. Goerbig, Quantum dimer models and effective Hamiltonians on the pyrochlore lattice, Phys. Rev. B **73**, 094430 (2006).

[58] B. Canals and C. Lacroix, Pyrochlore Antiferromagnet: A Three-Dimensional Quantum Spin Liquid, Phys. Rev. Lett. **80**, 2933 (1998).

[59] B. Canals and C. Lacroix, Quantum spin liquid: The Heisenberg antiferromagnet on the three-dimensional pyrochlore lattice, Phys. Rev. B **61**, 1149 (2000).

[60] J. H. Kim and J. H. Han, Chiral spin states in the pyrochlore Heisenberg magnet: Fermionic mean-field theory and variational Monte Carlo calculations, Phys. Rev. B **78**, 180410 (2008).

[61] F. J. Burnell, S. Chakravarty, and S. L. Sondhi, Monopole flux state on the pyrochlore lattice, Phys. Rev. B **79**, 144432 (2009).

[62] J. Oitmaa, C. Hamer, and W. Zheng, *Series Expansion Methods for Strongly Interacting Lattice Models* (Cambridge University Press, Cambridge, England, 2006).

[63] J. Oitmaa, R. R. P. Singh, B. Javanparast, A. G. R. Day, B. V. Bagheri, and M. J. P. Gingras, Phase transition and thermal order-by-disorder in the pyrochlore antiferromagnet $Er_2Ti_2O_7$: A high-temperature series expansion study, Phys. Rev. B **88**, 220404 (2013).

[64] L. D. C. Jaubert, O. Benton, J. G. Rau, J. Oitmaa, R. R. P. Singh, N. Shannon, and M. J. P. Gingras, Are Multiphase Competition and Order by Disorder the Keys to Understanding $Yb_2Ti_2O_7$?, Phys. Rev. Lett. **115**, 267208 (2015).

[65] R. Applegate, N. R. Hayre, R. R. P. Singh, T. Lin, A. G. R. Day, and M. J. P. Gingras, Vindication of $Yb_2Ti_2O_7$ as a Model Exchange Quantum Spin Ice, Phys. Rev. Lett. **109**, 097205 (2012).

[66] B. Tang, E. Khatami, and M. Rigol, A short introduction to numerical linked-cluster expansions, Comput. Phys. Commun. **184**, 557 (2013).

[67] Y. Huang, K. Chen, Y. Deng, N. Prokof'ev, and B. Svistunov, Spin-Ice State of the Quantum Heisenberg Antiferromagnet on the Pyrochlore Lattice, Phys. Rev. Lett. **116**, 177203 (2016).

[68] A. Smerald and N. Shannon, Theory of spin excitations in a quantum spin-nematic state, Phys. Rev. B **88**, 184430 (2013).

[69] V. K. Anand, L. Opherden, J. Xu, D. T. Adroja, A. T. M. N. Islam, T. Herrmannsdörfer, J. Hornung, R. Schönemann, M. Uhlarz, H. C. Walker, N. Casati, and B. Lake, Physical properties of the candidate quantum spin-ice system $Pr_2Hf_2O_7$, Phys. Rev. B **94**, 144415 (2016).

[70] A. Yaouanc, P. Dalmas de Réotier, C. Marin, and V. Glazkov, Single-crystal versus polycrystalline samples of magnetically frustrated $Yb_2Ti_2O_7$: Specific heat results, Phys. Rev. B **84**, 172408 (2011).

[71] K. A. Ross, Th. Proffen, H. A. Dabkowska, J. A. Quilliam, L. R. Yaraskavitch, J. B. Kycia, and B. D. Gaulin, Lightly stuffed pyrochlore structure of single-crystalline $Yb_2Ti_2O_7$ grown by the optical floating zone technique, Phys. Rev. B **86**, 174424 (2012).

[72] T. Taniguchi, H. Kadowaki, H. Takatsu, B. Fåk, J. Ollivier, T. Yamazaki, T. J. Sato, H. Yoshizawa, Y. Shimura, T. Sakakibara, T. Hong, K. Goto, L. R. Yaraskavitch, and J. B. Kycia, Long-range order and spin-liquid states of polycrystalline $Tb_{2+x}Ti_{2-x}O_{7+y}$, Phys. Rev. B **87**, 060408 (2013).

[73] O. Benton, Instabilities of a U(1) quantum spin liquid in disordered non-Kramers pyrochlores, Phys. Rev. Lett. **121**, 037203 (2018).

[74] R. Sibille, E. Lhotel, V. Pomjakushin, C. Baines, T. Fennell, and M. Kenzelmann, Candidate Quantum Spin Liquid in the Ce^{3+} Pyrochlore Stannate $Ce_2Sn_2O_7$, Phys. Rev. Lett. **115**, 097202 (2015).

[75] C. R. Wiebe and A. M. Hallas, Frustration under pressure: Exotic magnetism in new pyrochlore oxides, APL Mater. **3**, 041519 (2015).